



JOURNAL OF
APPLIED
CRYSTALLOGRAPHY

Volume 48 (2015)

Supporting information for article:

***In situ* X-ray Diffraction Environments for High-Pressure Reactions**

Bjarne R. S. Hansen, Kasper T. Møller, Mark Paskevicius, Ann-Christin Dippel, Peter Walter, Colin James Webb, Claudio Pistidda, Nils Bergemann, Martin Dornheim, Thomas Klassen, Jens-Erik Jørgensen and Torben René Jensen

Supporting information

Supporting information for the article “High-Pressure Gas-Solid Environments for *in situ* X-ray Diffraction”.

To illustrate the temperature gradient of the filament heater the following experiment was conducted. The heater was placed near a sapphire tube with an internal thermocouple. The heater was kept at a fixed temperature (140 °C), while the actual temperature was measured with a different thermocouple. The temperature was measured between the center of the coil and the edge of the coil. As shown in Figure S1 the temperature varies significantly with distance from the center of the coil. This indicates the importance of the careful alignment of sample, X-ray beam and thermocouple. Normally the heating filament is centered under the X-ray beam, which is hitting the sample 1-2 mm from the thermocouple. This may give rise to an error of ~ 8 % in the temperature.

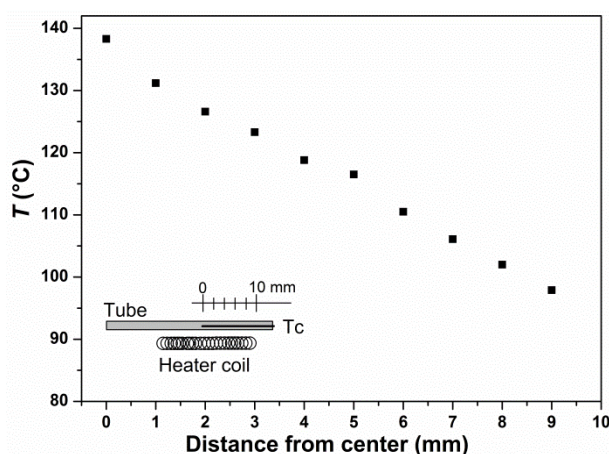


Figure S1 Filament heater temperature gradient. The filament was kept at a fixed temperature and with a K-type thermocouple the temperature was measured from the center to the edge of the filament heater coil. A linear temperature error of *ca.* 4 °C per mm is observed.

Figure S2

As an example, plots showing the calculated peak intensity over the total scattering from the sample, background and capillary are presented in Figure S2. The diffractogram of LaB₆ in the quartz tube is shown as the yellow line. First, the LaB₆ peaks are determined (red dots), followed by the background (black dots). The background is subtracted (Blue dots) and the peak profile is fitted using Gaussian symmetry (colored lines). Finally, the peak area is integrated, summed up and compare to the integral under the entire diffractogram which results in the peaks shown with blue dots. The grey inset in Figure S2(a) is shown in Figure S2(b) and provides a closer look at selected peaks. These steps were carried out using IPython and were performed for all tube materials and the “LaB₆ area : Total diffraction area” ratios are shown in Table 1.

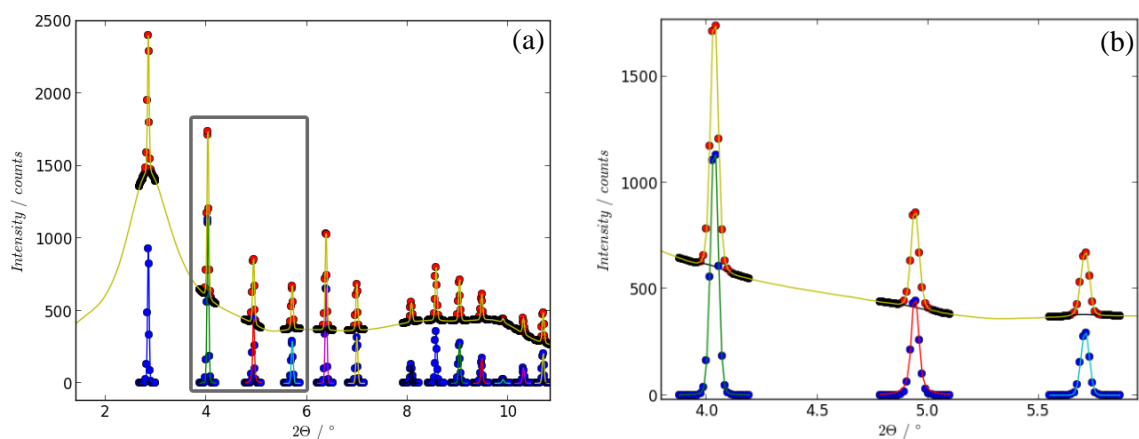


Figure S3 Diffractogram of LaB_6 in a quartz tube (yellow line) which give a visual example of how to determine the integral of the LaB_6 peaks and compare to the integral of the entire diffractogram. The inset in (a) is shown in (b) and provide a closer look at selected peaks.

Figure S3 shows the diffractogram of $\text{NaAlH}_4\text{-TiCl}_3$ (1:0.05) obtained at *RT* after each cycle step. As expected, the sample retains reversibility throughout the three hydrogen de- and absorption cycles.

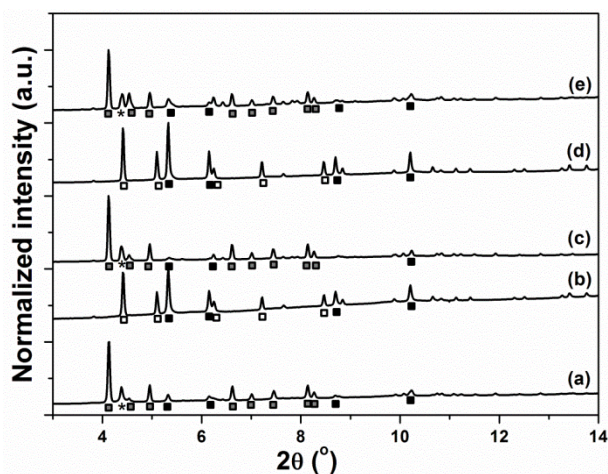


Figure S4 Diffractograms of $\text{NaAlH}_4\text{-TiCl}_3$ (1:0.05) obtained at *RT* after each cycle step, where (a) is after ball milling, (b) after first desorption, (c) first absorption, (d) second desorption and (e) second absorption. $\lambda = 0.2072 \text{ \AA}$, symbols: \blacksquare NaAlH_4 , \bullet Al , \square NaH , * TiCl_3 .